

AD-782 277

DELAYED FAILURE OF POLYCRYSTALLINE  
AND SINGLE CRYSTAL ALUMINA

R. J. Charles, et al

General Electric Research Laboratory  
Schenectady, New York

July 1962

DISTRIBUTED BY:

**NTIS**

National Technical Information Service  
U. S. DEPARTMENT OF COMMERCE  
5285 Port Royal Road, Springfield Va. 22151

AD782277

GENERAL  ELECTRIC  
*Research Laboratory*

①

REPORT NO. 62-RL-3081M

DELAYED FAILURE OF POLYCRYSTALLINE  
AND SINGLE-CRYSTAL ALUMINA

R.J. Charles and R.R. Shaw

July 1962

DDC  
RECEIVED  
MAY 16 1974  
RECEIVED  
B

Published by  
Research Information Section  
The Knolls  
Schenectady, New York

Reprinted by  
NATIONAL TECHNICAL  
INFORMATION SERVICE  
U. S. Department of Commerce  
Springfield VA 22151

SS

## ABSTRACT

This work was undertaken to confirm and extend prior work on the static fatigue or delayed failure of alumina ceramics. The investigations were particularly concerned with the effects of water vapor and temperature on the long-term mechanical strengths of these materials. Mechanical tests were therefore made over a large temperature range ( $-196^{\circ}$  to  $1100^{\circ}\text{C}$ ) in dry, humid, and saturated atmospheres.

Both single-crystal sapphire and polycrystalline alumina exhibited strong delayed failure characteristics which depended on atmosphere, temperature, and strain rate. Delayed failure was absent at liquid nitrogen temperatures, most readily observable around room temperature and decreased with further increases of temperature until at  $900^{\circ}\text{C}$  it was no longer observable. A very rapid decrease of observed strength of the ceramics with increasing temperature (to  $900^{\circ}\text{C}$ ) was observed. This reduction in strength, however, cannot presently be attributed to a corrosion fatigue effect.

A fatigue theory involving stress corrosion of an elastic continuum has been applied to the low-temperature experimental data on sapphire. Reasonable values for the parameters involved in the theory were obtained.

Manuscript received June 29, 1962.

# DELAYED FAILURE OF POLYCRYSTALLINE AND SINGLE-CRYSTAL ALUMINA †

R. J. Charles and R. R. Shaw

## INTRODUCTION

Task 9 consisted of a study of the corrosion processes which affect the long-term strength of single-crystal and polycrystalline aggregates of  $Al_2O_3$ . It was desired to obtain information on the identity of the corrosion reactions, their mechanisms, and their effect upon the rupture strength of these ceramics.

The most noticeable effect of delayed failure, or "static fatigue," is the sharp dependence of observed strength upon the atmosphere present during the performance of the test. Another related effect is the decrease in resistance to failure with decrease in the rate of loading in certain atmospheres, i. e., the observed strength is lower the longer it takes to apply the breaking load. At zero rate of loading (deadweight loading), the observed strength should be at a minimum, and times-to-failure under a given set of external conditions may be measured.

Much work along these lines has been done on inorganic glasses. Oxide glasses are nearly ideal materials for study of this kind because of their homogeneity, isotropy, and brittleness. Delayed failure has been found to depend heavily on strain rate, temperature, pressure, atmosphere, surface condition, composition, and prior thermal history.

Very little work has been done, however, on crystalline oxides. Among the first references to the delayed failure effect in crystalline oxides was that of Roberts and Watt, <sup>(1)</sup> who noted in 1949 that sintered alumina test specimens failed at 5 minutes and 120 minutes after loading in tension. Wachtman and Maxwell, <sup>(2)</sup> working in air with single-crystal sapphire, found a delayed fracture effect in most of the dozen samples tested at room temperature. Williams, <sup>(3)</sup> working with a low-density (3.84 g/cc) sintered alumina body, found times-to-failure in air as long as  $10^5$  seconds, depending on the stress level applied. Pearson, <sup>(4)</sup> also working with rather low-density sintered alumina, found that delayed

---

†Submitted to Armour as "Final Report of Task 9 of Studies on the Brittle Behavior of Ceramic Materials--Delayed Failure of Polycrystalline and Single Crystal Alumina."

fracture effects in ordinary atmospheric conditions could be largely eliminated by heating to about 350°C, cooling, and testing, all under a vacuum of less than 10<sup>-5</sup> mm Hg. From this it was concluded that the effect was caused by an unspecified atmospheric attack acting on Griffith flaws in the stressed material.

All of the above investigations were done at room temperature. At other temperatures, Brenner<sup>(5)</sup> statically loaded sapphire whiskers at 1100° and 1450°C in dry H<sub>2</sub> and found no evidence of delayed failure; these results were inconclusive, however, since the load was only one-third to two-thirds of the dynamic failure stresses, and the times were relatively short. Later work in both hydrogen and oxygen atmospheres demonstrated fatigue in whiskers, however, with the time to fracture being exponentially related to the applied stress. Charles<sup>(6)</sup> has reported work on oxides including fused silica, granite, albite, spodumene, hornblende, sapphire, quartz, and magnesium oxide. This work included both crossbend tests on sapphire and compression tests on the other oxides, done in atmospheres of nitrogen-water combinations over a temperature range of -200° to 240°C. It was shown that minimum strength values were obtained with a simultaneous application of stress and corrosive atmospheres. Atmospheres alone had little weakening effect on stress-free material, even MgO. Of great interest was the appearance of a definite strain-rate dependency of the failure stress.

In summary, it is clear that both polycrystalline and single-crystal alumina exhibit static fatigue in normal atmospheres. It is not clear, however, whether MgO, either in single or polycrystalline form, exhibits behavior which may be characterized correctly as static fatigue. It seems<sup>(6)</sup> that MgO hydrates readily and that hydration with simultaneous plastic deformation can lead to low rupture strengths. Since it has been, however, the experience of these authors, and others,<sup>(7)</sup> that standard dead load tests on single-crystal MgO specimens under ordinary conditions do not give evidence of static fatigue, this material was not included for study under the Task 9 program.

#### EXPERIMENTAL APPROACH

To determine whether or not a delayed failure or fatigue effect exists in a given material, it is generally useful to obtain "base level" data, gathered in the absence of fatigue, against which comparisons of failure strengths under ordinary conditions may be made. The possibilities which exist for gathering base level data include the following:

1. Using low temperatures to inhibit the temperature-dependent kinetic factors which govern reaction rates.

2. Maintaining atmospheric conditions such that an atmospheric reaction cannot occur, i. e., vacuum or inert atmospheres.

3. Using a very fast loading rate.

For a given group of specimens, with equivalent severity of surface notches or micro-cracks, destructive tests may be made under various conditions of load, time, and environment and the failure strength values compared against a maximum strength obtained under one of the above base level conditions. In this manner the severity of the fatigue effect may be estimated.

#### Dynamic and Static Testing

Obviously, if fatigue does not occur, the strength of a sample is dependent only on stress level and not at all on time. Conversely, if fatigue occurs, the failure strength or observed strength will be a complex function of the time of load application and the load changes, if any, during testing. Thus, in principle fatigue data can be obtained from tests at constant load or constant strain rate.<sup>(6)</sup> Both techniques were used in the experimental work described here.

#### Atmospheres and Temperatures

It is apparent that water vapor is one of the most influential atmospheres which cause fatigue in oxides. The reaction is generally the formation of a hydrate. In the case of alumina, the specific hydrate formed is a function of temperature and pressure, with water or (OH<sup>-</sup>) groups being lost as temperature increases.

Thus, if the hydration reaction is important in fatigue of alumina, one would expect to emphasize the delayed failure effects by conducting tests at moderate or low temperatures wherein mono- or multilayer adsorptions of water vapor are readily obtainable (i. e., the vapor pressure of water should be at least 0.4 times the saturation water vapor pressure for the temperature considered). These considerations led to a selection of an experimental temperature range for static testing from -55° to about 200°C wherein fatigue effects due to hydration could be studied.

It is conceivable that mechanisms dependent on the reduction, by hydrogen, of alumina to suboxides could result in static fatigue. Such a reduction reaction is known to result in the formation of alumina whiskers at high temperatures and it is possible that similar mass transport processes may change micro-crack geometries such that a

stressed specimen may experience a time dependent failure. For these reasons it was considered necessary to perform further experiments with alumina at temperatures in excess of 800°C in hydrogen atmospheres to determine whether or not a reduction reaction could lead to fatigue. Vacuum tests at these temperatures allowed estimates of the severity of the fatigue effect to be made, as mentioned before.

## EXPERIMENTAL MATERIALS

The specimens used in this investigation were both single-crystal and polycrystalline alumina.

### Sapphire

The sapphire single crystals used were obtained from the Linde Company, and consisted of random lengths of ground rod from which specimens of appropriate size were prepared. The diameter of these specimens was  $0.070 \pm 0.0003$  inch. To insure that proper correlations between these specimens and the 0.125-inch specimens used throughout the other Tasks could be made, a number of these larger specimens were obtained and their bend strength values were compared with the 0.070-inch material. Correlations were exact within a few per cent.

The use of such single crystals in a research program presents certain special problems. The material itself is made by the Verneuil process, and is rarely completely free of the spherical gas bubbles which are trapped during the process. Careful selection of specimens must be made to exclude such faulty material. Internal strains are to be expected due to the discontinuous manner in which material is added to the growing boule. Annealing after manufacture (details unavailable) is done to help lessen the effect of these strains. And, finally, the individualistic nature of each rod must be taken into account, for each rod experiences somewhat different conditions during its growth, such as temperature fluctuations and different seed stock. Because of all these inherent sources of nonuniformity, it was decided to use numerous individual rods in each test and take their average, rather than try to compare the properties of individual rods under a given range of conditions.

Sapphire presents further problems because of its anisotropy. In bending, the effect of specimen orientation with respect to the optic axis is especially important; it has been reported<sup>(8)</sup> that loading parallel to the optic axis results in observed strengths nearly three times as high as loading perpendicular to the axis. It was decided to use one standard orientation throughout testing, with the load applied perpendicular to the intersection of the neutral surface with the basal plane, which intersection

was in turn perpendicular to the specimen rod axis (Fig. 1). This position corresponds to a maximum extinction position in polarized light when the rod axis is parallel to the vibration direction of one of the crossed polarizing prisms.

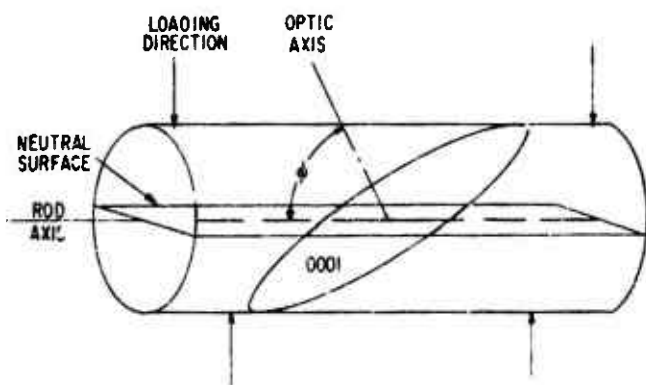


Fig. 1 Load geometry for sapphire single crystals.

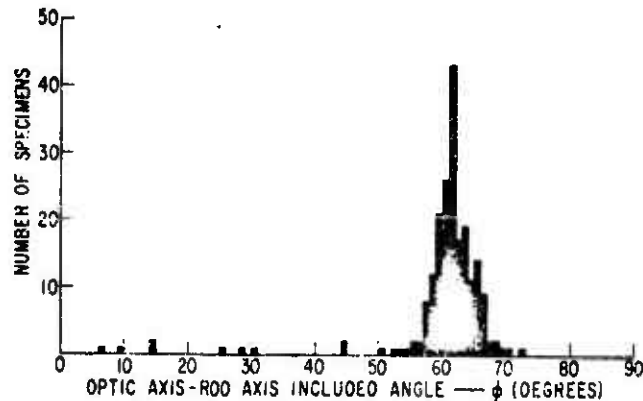
No account was taken of the test orientation with respect to the second-order prism axes  $a_1$ ,  $a_2$ , and  $a_3$ , i. e., the  $3L_2$  axes. These axes correspond with the direction of basal slip in the material, which is important at higher temperatures in producing plastic flow and fracture. This investigation, however, was concerned only with brittle fracture at temperatures generally well below those required for plastic deformation at the strain rates employed. In addition, experimental work<sup>(8)</sup> indicates that little or no effect of  $L_2$  axis orientation on the observed low-temperature bend strength can be observed. Thus the angle  $\phi$ , with the optic axis in the plane of bend, was taken as the only critical parameter.

Boules grown by the Verneuil process as a rule do not have their optic axis parallel to the boule axis, and similarly the rods made from them have their optic axes tipped at some angle from the rod axes. The effect of the growth angle on mechanical properties is quite large, as seen by modulus of rupture values reported by Seemann<sup>(9)</sup> and the Linde Company (Table I; test conditions unknown). The angle is usually measured as  $\phi$ , the angle between the optic axis (normal to the basal plane 0001) and the longitudinal rod axis. The preferred growth direction is near  $60^\circ$  according to the manufacturer. In order to check the orientations of incoming samples, a device was constructed to orient the samples by optical principles and to obtain values of  $\phi$ . Some specimens were also oriented by x-ray techniques, partly as a check on the optical equipment. Figure 2 demonstrates the angular distribution of  $\phi$  for some 360 samples checked during the investigation. This

TABLE I  
Reported Room Temperature  
Bend Strength Data for Sapphire [Seemann<sup>(9)</sup>]

$\phi$	Modulus of Rupture
30°	100,000
45°	78,000
60°	65,000
75°	94,000

Fig. 2 Optic axis orientations for sapphire test specimens.



distribution is similar to that of Wachtman and Maxwell<sup>(2, 10)</sup> whose "χ" is the complement of  $\phi$ . Only those samples falling in a range of 58°-68° were used in this investigation. It is of interest that some 15 per cent of the off-the-shelf samples received from the manufacturer were rejected in this manner; this percentage of nonstandard specimens could seriously affect the results of almost any testing program.

All specimens were cleaned before testing to remove oil from the skin, dust, immersion oils, and other contaminants. The cleaning process was a series of baths of toluene and acetone, interspersed and concluded with distilled water rinses. Specimens were dried and stored in cardboard until ready for use.

#### Polycrystalline Alumina

Lucalox<sup>†</sup> alumina was used for the fatigue experiments. The type of testing done by this Task required a different specimen size and

<sup>†</sup> Trade-mark of General Electric Company.

shape from the dog-bone type. Therefore, polycrystalline samples were extruded to order, prefired, and finally sintered to the requisite degree of density and strength. Pains were taken to insure that the rod specimens used had the same surface grain size and strength characteristics as the specimens used in the other investigations. In order to do this, some preliminary work was done on the relationship between the density, grain size, and observed four-point bend strength of polycrystalline alumina.

All polycrystalline material was tested in the as-fired condition. No particular preparation of the surface was made, other than the pretest cleaning by consecutive washes in toluene, distilled water, acetone, and distilled water, as above.

## EXPERIMENTAL EQUIPMENT

The equipment and fixtures used in this investigation were designed to test the material in two ways: dynamic bending and static bending.

### Dynamic Bending

Dynamic bending consisted of four-point bending with a constant strain rate applied to the gage section of the specimen. Four-point bending was selected because of the constant bend moment it provides across the inner span. Because of the brittle nature of the specimens, and their small deflections prior to fracture, the usual expression for stressing load beams was used, i. e. ,  $\sigma = \frac{Mc}{I}$  , where

$\sigma$  = failure stress at outer fiber

M = bending moment

c = distance from outer (tension) fiber to neutral axis

I = section moment of inertia.

An Instron testing machine was fitted out to allow dynamic tests at temperatures up to 1150°C in various neutral or reducing atmospheres. This consisted of a molybdenum bend fixture which could be used in air or encased within a stainless steel jacket for other atmospheres. A triple-wound Kanthal furnace surrounding the jacket provided heat for the higher temperatures, and a Styrofoam case surrounding the jacket permitted low temperature tests using liquid nitrogen. Temperature in all cases was controlled by three Chromel-Alumel thermocouples within the bend fixture itself, and could be held to within  $\pm 10^\circ\text{C}$  of the nominal temperature at all temperatures.

In view of the large number of tests required for the program, it was decided to construct a fixture to permit testing of up to 20 specimens per run, in the temperature range mentioned previously. Figure 3 demonstrates the action of the molybdenum fixture which resulted. Specimens are loaded at four points as the outer fixture moves past the inner one. Loading spans are 1.20 x 0.70 inch, respectively. Various modifications have not changed the principle of the apparatus. During tests involving sapphire, orientation was achieved by winding the specimens with three wraps of 0.010-inch nickel wire, and allowing the weight of the wire to keep the specimen oriented correctly. Effect of the wire on specimen strength was apparently negligible. Fracture seldom occurred at the point of wire contact.

Vacuum atmospheres to  $10^{-5}$  mm Hg were provided by mechanical pumps and an oil diffusion pump, and were measured by a cold cathode gage. "Wet" hydrogen atmospheres and saturated air atmospheres were provided by bubbling these line gases through several water bubblers and a detraining flask. Dry hydrogen atmospheres were produced first by using commercial pure tank hydrogen, but later on dry hydrogen was

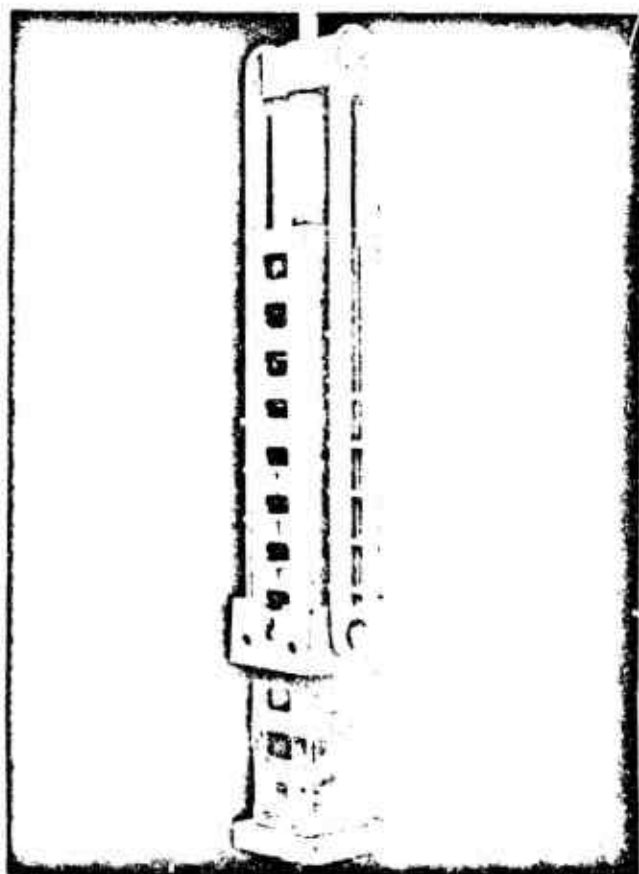


Fig. 3 Molybdenum  
high-temperature test  
apparatus.

produced by putting line hydrogen through oxygen, liquid nitrogen, and desiccant traps. The measured dewpoint was  $-46^{\circ}\text{C}$ , corresponding to a water vapor concentration of  $5 \times 10^{-5}$  mols/liter.

### Static Bending

Static bending consisted of four-point bending with a constant stress applied to the gage section following a nearly instantaneous loading. This was accomplished in the apparatus shown in Fig. 4. The heating jacket shown on the autoclave permitted the use of saturated steam atmosphere up to 200 psi. Ten specimens at a time can be tested in this fixture. A relay-contact system permits times-to-failure to be read directly from the series of clocks shown, to an accuracy of  $\pm 5$  seconds. A Styrofoam jacket permits testing in any atmosphere down to  $-150^{\circ}\text{C}$ , using liquid nitrogen.

Weights may be adjusted to permit any stress level desired to be applied to the specimen. Outer and inner spans are 3.75 and 1.0 inch, respectively.

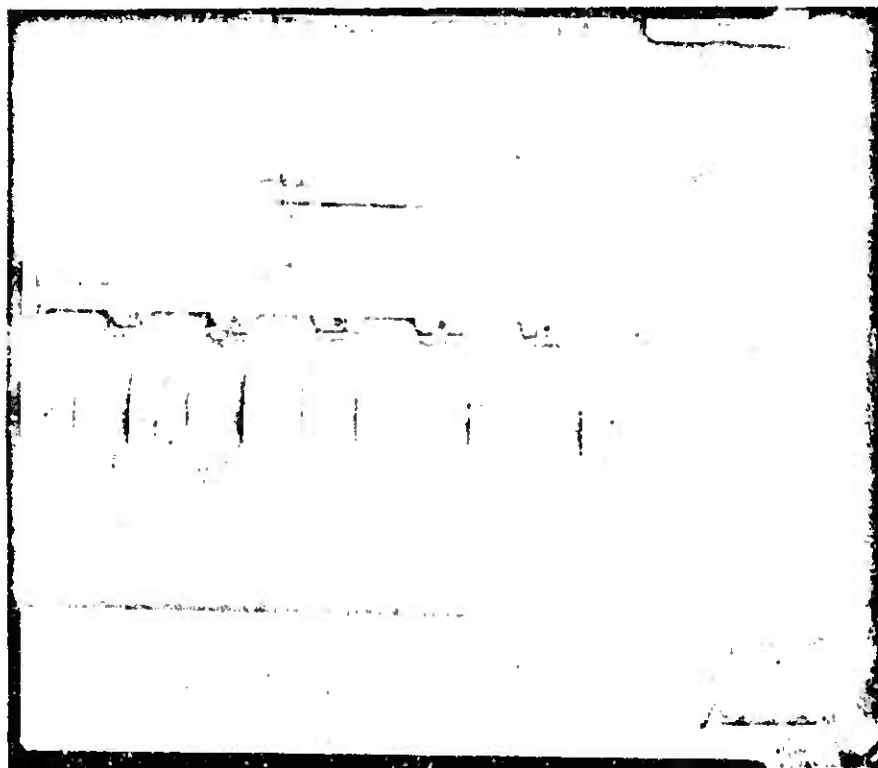


Fig. 4 Low temperature autoclave test apparatus.

## EXPERIMENTAL RESULTS FOR SINGLE-CRYSTAL ALUMINA

### 1. Condition of Specimens

The marked anisotropy of sapphire monocrystals mentioned earlier required a certain standard orientation to make comparative results meaningful. Another effect of this anisotropy is the variable resistance to wear or abrasion which different crystallographic planes and directions exhibit. Steijn<sup>(11)</sup> has shown experimentally that resistance to wear of the basal plane can be nearly two orders of magnitude lower than that of the prismatic and rhombohedral planes. In particular, it is shown that the rate of wear of sapphire rods is some 30 times greater for "ninety-degree" material ( $\phi = 90^\circ$ ) oriented for attack on the basal plane than for zero-degree material oriented on prismatic planes. This is indicated schematically in Fig. 5.

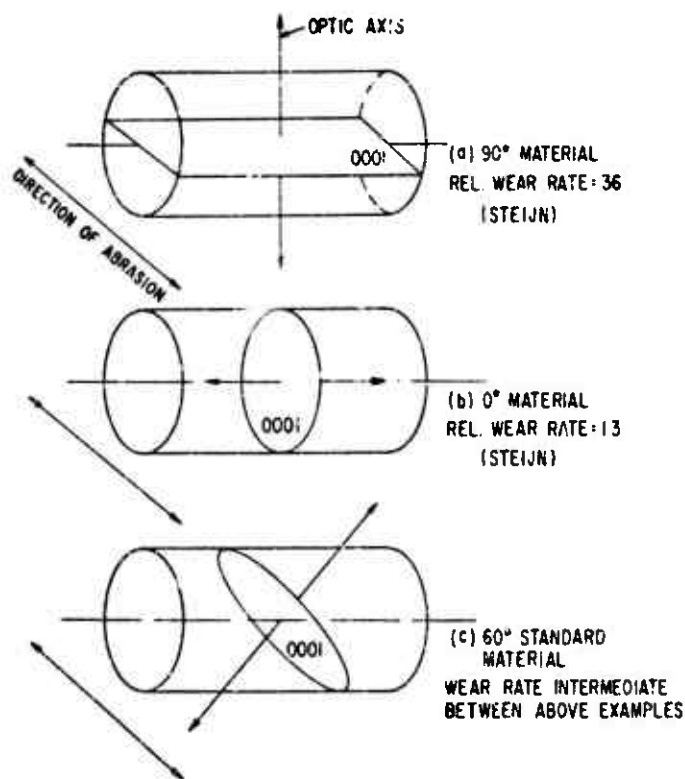


Fig. 5 Relative wear rates of sapphire rods of various orientations.

The standard material used in the present investigation is around  $60^\circ$ , so that its wear rate in the orientation illustrated is intermediate between the two extremes. This means that during the centerless grinding of sapphire rods the grinding rate will be increased

when the rods come into this relative orientation with the grinding rolls. The result is that the rods will not be ground round in cross section.

This effect was quite noticeable in the present work. Under medium reflected light and at the proper viewing angle, "flats" or bright bands on the as-ground rods can be easily detected on opposite sides of the rod. This amounts to a diameter difference of 0.2 to 0.4 mil, which is usually within the specified tolerance of the rod as supplied. Thus the gross geometrical effect on the rod is negligible. However, the effect on a microscopic scale may be more serious, for the areas of greatest grinding attack are also the top (compression) and bottom (tension) surfaces of the specimens when in the standard test orientation. No attempt was made in this investigation to find the real significance of this effect; all data are uncorrected for it.

### 2. Effect of Thermal History

Jackman and Roberts, (12) and Wachtman and Maxwell, (13) noted that the observed bend strength of sapphire monocrystals at first declined with increasing temperature, and then rose again at temperatures near 1000°C. Also, Tomilovskii<sup>(14)</sup> found that heat treatments of sapphire prisms to temperatures of 1300°C produced a 30 to 40 per cent increase in the observed bend strength, measured at room temperature. In both cases the effects were ascribed to high-temperature relief of internal stresses which had been introduced during manufacture.

Both of the above observations were confirmed in the present test work, indicating that the observed strength of sapphire is very sensitive to its prior thermal history. Figure 6 shows the dependence

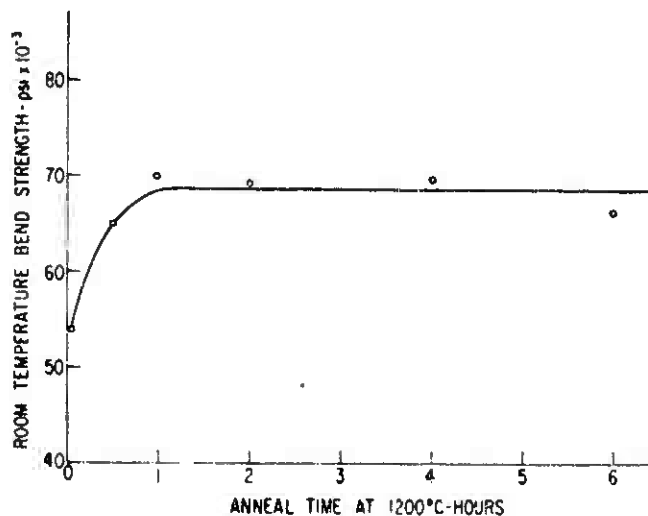


Fig. 6 Effect of anneal time at 1200°C on bend strength of sapphire single crystals.

of observed bend strength of as-received sapphire rods at room temperature on annealing time at 1200°C in air. It is seen that the "annealing" mechanism operates fairly quickly at this temperature, with the bend strength reaching its maximum value in a few hours. Longer heat treatments (out to 6 hours) produced less scatter. Results of various annealing tests are presented in Table II. The atmosphere during the heat treatment apparently has little effect on the final mechanical properties, at least at the temperature studied.

TABLE II  
Effect of Heat Treatment of Sapphire on  
Bend Strength at Room Temperature

<u>Original Strength (psi)</u>	<u>Temp (°C)</u>	<u>Time (hr)</u>	<u>Atmosphere</u>	<u>Final Strength (psi)</u>	<u>% Increase</u>
65,000	1300	1 to 6	Air	87,600	35 <sup>(15)</sup>
59,200	1000	4	Vacuum	92,200	56*
54,000	1200	1 to 6	Air	69,000	28
71,000	1125	6	Air	100,000	40†
			Wet H <sub>2</sub>		
			Dry H <sub>2</sub>		
			Vacuum		
			Dry N <sub>2</sub>		

\*All tests in vacuum.

†All tests in liquid N<sub>2</sub>.

### 3. Base Level Strength of Sapphire

Because of the sensitivity of sapphire to its prior thermal history, it was decided to conduct parallel tests on both "as-received" material and samples heat treated at 1200°C for 6 hours in air. These two sets of samples will be referred to as "as-received" and "annealed," respectively, throughout this report. Table III lists the liquid nitrogen and room temperature bend strengths of sapphire crystals in which the base planes exhibited two different orientations to the specimen axes.

TABLE III  
Effect of Temperature and Basal Plane Orientation on  
 Observed Bend Strength of Sapphire

<u>Orientation</u>	<u>As-received</u>			<u>Rupture Strength (psi)</u>
	<u>No. Tests</u>	<u>Temp (°C)</u>	<u>Test Atmosphere</u>	
Zero-degree 0.070 in. diam	10	25	Air	102,000
Zero-degree 0.070 in. diam	20	-196	Liq. N <sub>2</sub>	170,000
60° 0.070 in. diam.	9	25	Air	54,600
60° 0.070 in. diam.	35	-196	Liq. N <sub>2</sub>	71,000
60° 0.125 in. diam.	11	25	Air	59,800
60° 0.125 in. diam.	9	-196	Liq. N <sub>2</sub>	75,100
	<u>Annealed</u>			
Zero-degree 0.070 in. diam.	3	-196	Liq. N <sub>2</sub>	175,000
60° 0.070 in. diam.	35	-196	Liq. N <sub>2</sub>	100,000
60° 0.070 in. diam.	35	25	Air	69,000

It will be noted that the strength of the zero-degree rods is approximately twice that of the 60° specimens at both temperatures for the as-received material. This shows a very real effect on strength of variation of the angle  $\phi$ , as discussed earlier. The close correlation of strength of the two different sizes of specimens is also evident.

Annealed zero-degree material is still stronger than annealed 60-degree stock, but not by as wide a margin as in the as-received specimens. In fact, there seems to be little or no change in the observed liquid nitrogen strength of zero-degree sapphire on annealing. This indicates that: (1) either the zero-degree material has had a full anneal before leaving the manufacturer, or (2) its unique crystallographic orientation masks any thermal effects.

The base-level strengths of sapphire are then taken to be 71,000 and 100,000 psi for as-received and annealed 60° specimens, respectively.

#### 4. Constant Strain-Rate Tests on Sapphire

Figure 7 presents the behavior of as-received sapphire rods in four-point bending in various atmospheres and at various temperatures. Each point represents the average of 10 to 20 samples, tested at an outer-fiber strain rate of  $3 \times 10^{-4}$  in/in/min. "Wet" hydrogen refers to hydrogen saturated at room temperature with water.

Several things are of immediate interest from these data. First, at temperatures up through 850°C the bend strength diminishes in the order of vacuum, dry hydrogen, and wet hydrogen atmospheres. Thus strength decreases as the atmosphere becomes more reactive chemically, which is one of the main predictions of a stress-corrosion hypothesis. Second, the reported<sup>(12, 13)</sup> strength minima at intermediate temperatures occur. Third, the differences in observed strength in the various atmospheres decreases with increasing temperature, indicating that the fatigue effect is lessening. Above 900°C there is no apparent effect.

At 1000°C plastic deformation of the samples was evidenced by deflections in the load-time curves; no equilibrium flow stress was reached before fracture. Extrapolated data from a recent paper by Kronberg<sup>(15)</sup> on strain-rate effects in sapphire indicate that the maximum strain rate to observe an initial yield point in sapphire is about  $5 \times 10^{-5}$  in/in/min at 1000°C, about two orders of magnitude less than the strain rate actually used. However, at 1150°C the maximum strain rate plotted from Kronberg's data is the same as the strain rate used here. Thus it seems quite plausible that the extraordinarily high strength of as-received sapphire at 1000°C is permitted by localized stress relief by plastic deformation.

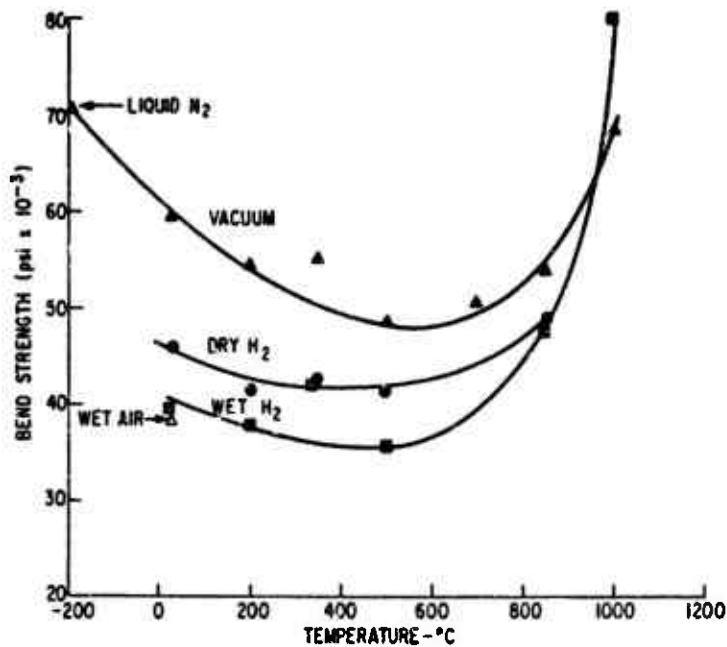


Fig. 7 Temperature-atmosphere effects on the bend strength of as-received single-crystal sapphire.

Figure 8 represents the behavior of annealed sapphire rods as before. Each point represents the average of 4 to 5 tests.

It is seen that these are fundamentally different plots. No minima are evident in Fig. 8, and the stress values are very much higher. The order of decreasing strength in the various atmospheres is preserved to about 850°C. As before, the strength differences decrease with temperature, becoming negligible at 850°C. No attempt was made to perform comprehensive tests at higher temperatures because of the observed plastic flow which defeats the study of brittle fracture.

Figure 9 gives perspective on the behavior of both the "as-received" and "annealed" varieties of sapphire tested. Their behavior is that of two different materials up to a temperature of about 850°C, above which mechanisms of plastic flow take over at the strain rate used.

Figure 10 illustrates the normalized vacuum strength of sapphire as a function of temperature and the normalized Young's modulus of sapphire over the same temperature range. Both are approximately linearly dependent upon temperature, but it is seen that the observed strength for sapphire single crystals is much more strongly affected by temperature increases than is the Young's modulus. This is not the case with polycrystalline material, as will be shown later.

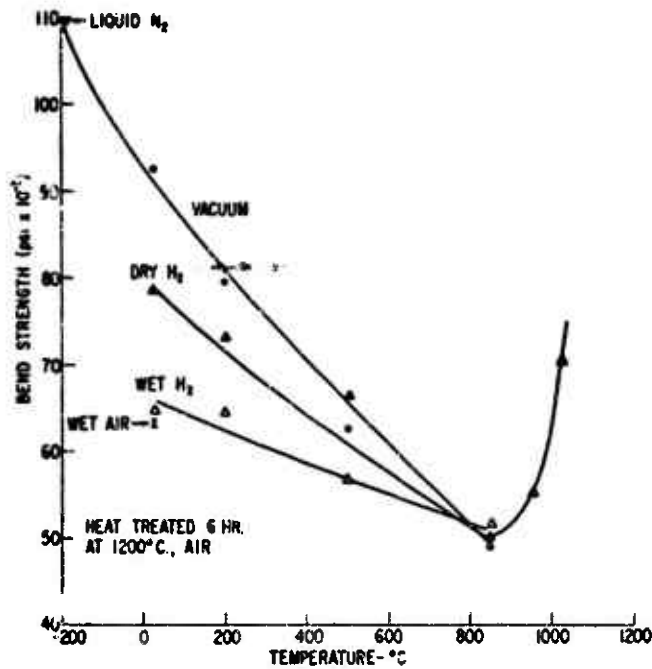
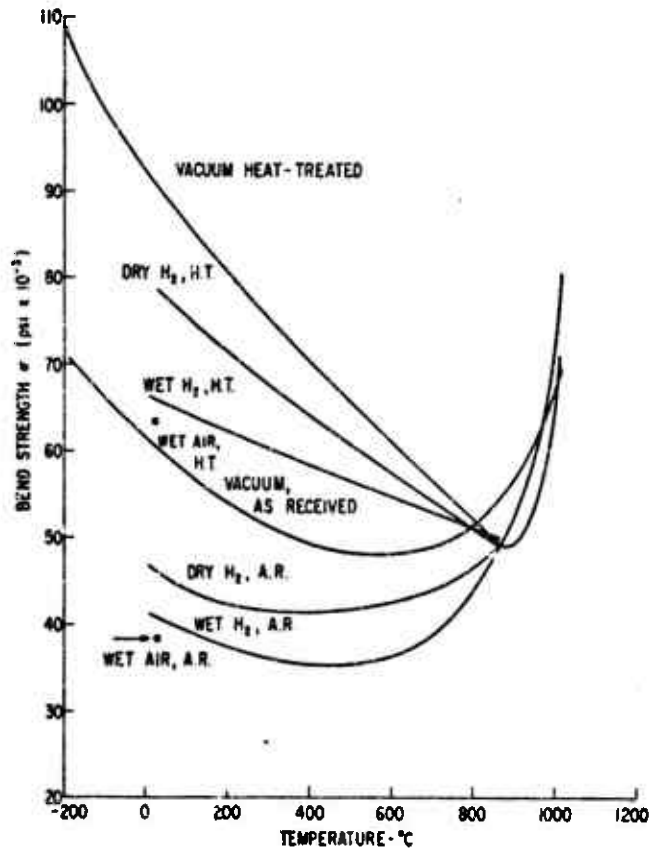


Fig. 8 Temperature-atmosphere effects on the bend strength of heat-treated single-crystal sapphire.

Fig. 9 Comparison of bend strengths of as-received and annealed single-crystal sapphire.



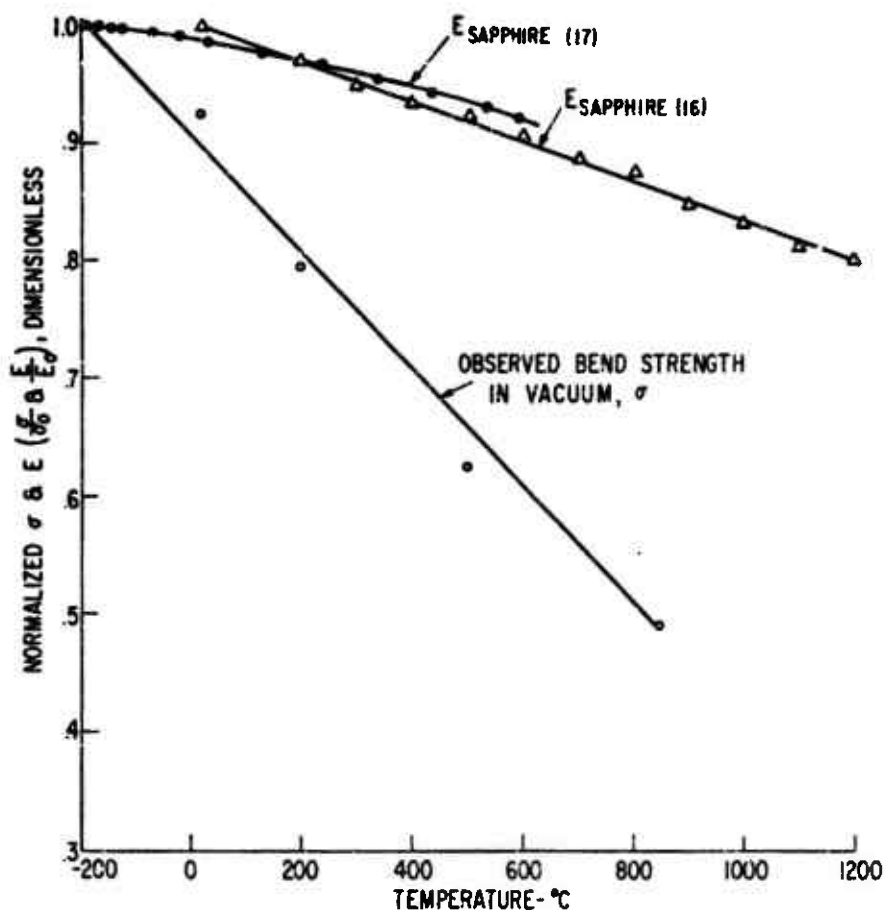


Fig. 10 Annealed sapphire single-crystal bend strength and Young's modulus vs temperature.

### 5. Delayed Failure Tests on Sapphire

Table IV lists times-to-failure data for various conditions for sapphire specimens under static load. Figure 11 is a plot of the observed breaking stress (normalized on the base level stress) vs times-to-failure. No complete curve for any one temperature could be obtained, because the median times-to-failure were either forbiddingly long at low stresses for the low-temperature segment, or were impossibly short to measure at high stresses for the high-temperature segment. The temperature dependence of the apparent corrosion process is obviously quite strong.

TABLE IV  
 Static Fatigue Data for Single-Crystal Sapphire

Constant Stress ( $\sigma$ )	Conditions	No. Specimens Failing Within Indicated Time Decades (minutes)										Most Prob. Time-to- failure (min)			
		$10^{-2}$	$10^{-1}$	$10^0$	$10^1$	$10^2$	$10^3$	$10^4$	$10^5$	$10^6$	$<10^4$				
41,600 psi	T = 190°C. 200 psia steam	10													~ 0
23,500 psi	As above	6	3	11	12	3									3
20,500 psi	As above		1	4	14	7	2	7							90
18,400 psi	As above		4	5	10	12	7	3	1000						1000
16,800 psi	As above				3	1	1	1							--
34,400 psi	T = -35°C. Sat. water vapor	2		15	5	5	3	5	7						7
39,000 psi	As above			0	2	1									--
46,100 psi	As above	7	4	9	1	1									0.5
34,400 psi	Room Temp. Sat. water vapor	8	1			1									--
53,400 psi	T = -35°C. Sat. water vapor	15	9	1	2	1									0.02

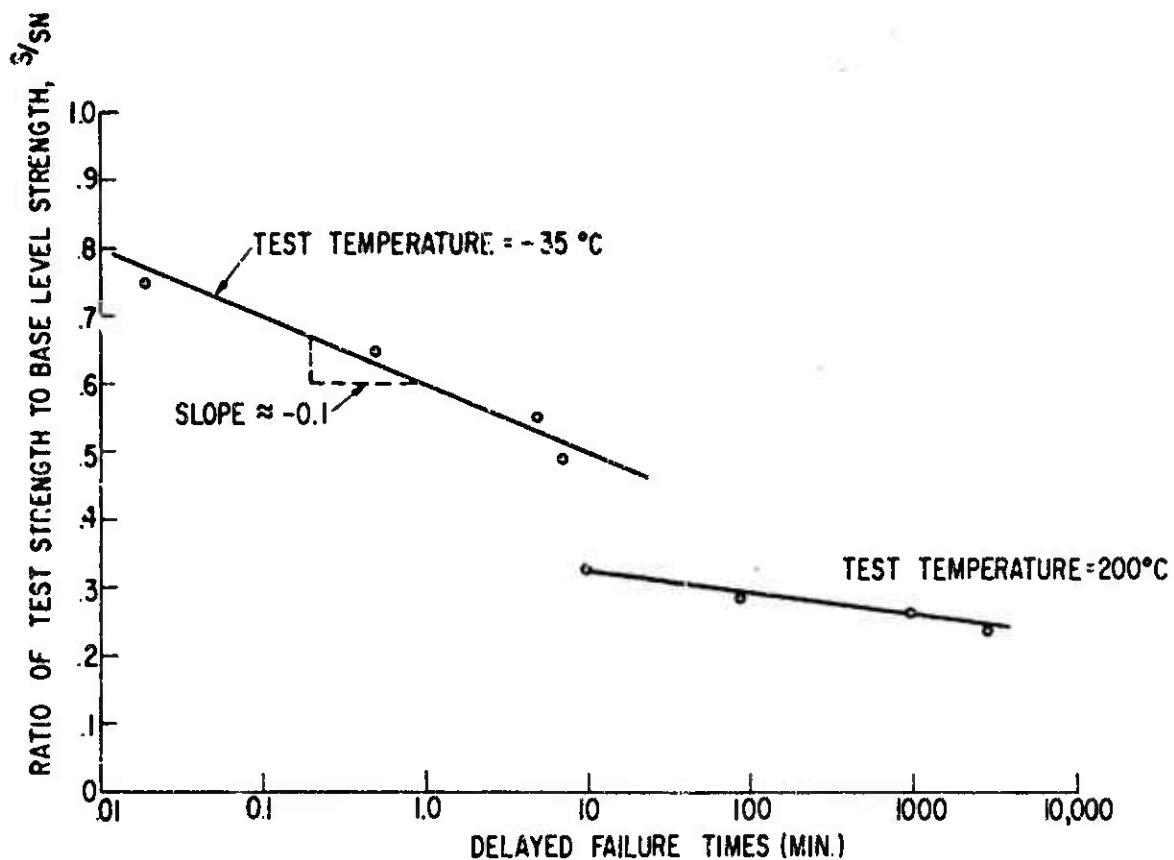


Fig. 11. Static fatigue curve for single-crystal sapphire.

## 6. Sapphire Fracture Surfaces

It might be expected that a stress-corrosion mechanism would affect the mode of fracture, which could be detected by examining the fracture surfaces.

Pigolina *et al.*<sup>(18)</sup> and Winchell<sup>(19)</sup> have investigated fracture modes of sapphire crystals. Their work shows that the first- and second-order prism planes, basal plane, and rhombohedral planes are the common parting planes. Of these, the basal and rhombohedral  $(10\bar{1}2)$  faces have the highest degree of development, possibly indicating that these planes are most susceptible to parting during fracture. Petch<sup>(20)</sup> suggests that "interrupted cleavage" may occur on basal, prismatic, and bypyramidal  $(11\bar{2}2)$  planes.

Examination of the fracture surfaces produced during this program indicates that a considerable variation in fracture behavior can

be induced by varying the test conditions. Failure under static load in a water vapor atmosphere at 200°C, for example, almost invariably produces a bright curved mirror surface, completely free of markings. The identical test at -35°C, produces almost no mirror surfaces, and conchoidal surfaces with a horde of checks, steps, rivulets, etc., predominate. At room temperature an intermediate appearance obtains. Occasionally minor cleavage or parting occurs along definite crystallographic planes; x-ray analysis determines these planes to be (10 $\bar{1}$ 2).

Failure under a dynamic load operates in a similar manner. Zero-degree material commonly fractures along (10 $\bar{1}$ 2) at room temperature in air, but in liquid nitrogen it is extremely rare to find a planar fracture. Standard material fracture surfaces showed the effect of both temperature and atmosphere: tests conducted in wet hydrogen at all temperatures generally produced more mirror surfaces than in dry hydrogen; dry hydrogen and vacuum testing produced generally rough, featureless fracture surfaces, with a few planar facets showing.

## EXPERIMENTAL RESULTS FOR POLYCRYSTALLINE ALUMINA

### 1. Strength vs Grain Size and Testing Rate

Figure 12 represents the results of the preliminary grain size-strength investigation mentioned earlier. Each point represents 20 to 30 individual tests, performed at a constant strain rate of 1.4 (10<sup>-2</sup>) in/in/min, in air at room temperature, on as-fired specimens. Span lengths varied from 1.25 x 0.25 to 1.50 x 0.68 inch to accommodate the different diameters of the varying batches of material, which were generally about 65 mils. This was necessary to preserve the constant strain-rate feature. Density was measured by standard displacement methods. The method of obtaining "grain size" was to use lineal analysis on the surface layers of the specimens, with the average grain size  $\bar{D}_{avg} = \frac{3}{2} \bar{l}$ , where  $\bar{l}$  is the mean traverse length.<sup>(21)</sup> All measurements were taken from photomicrographs.

Figure 12 shows that the material is reasonably well-behaved and may be reproduced. Essentially full density is achieved above 30-micron grain size. The lower-density material may be likened to high-purity commercial alumina, with the reservation that the grain size is more uniform in the Lucalox alumina. An exception to this was the single point shown at a nominal grain size of 66 microns. This particular batch of material had experienced rather severe discontinuous grain growth during processing, and had a very broad grain size distribution. Some surface grains were as large as 200 microns. To preserve consistency

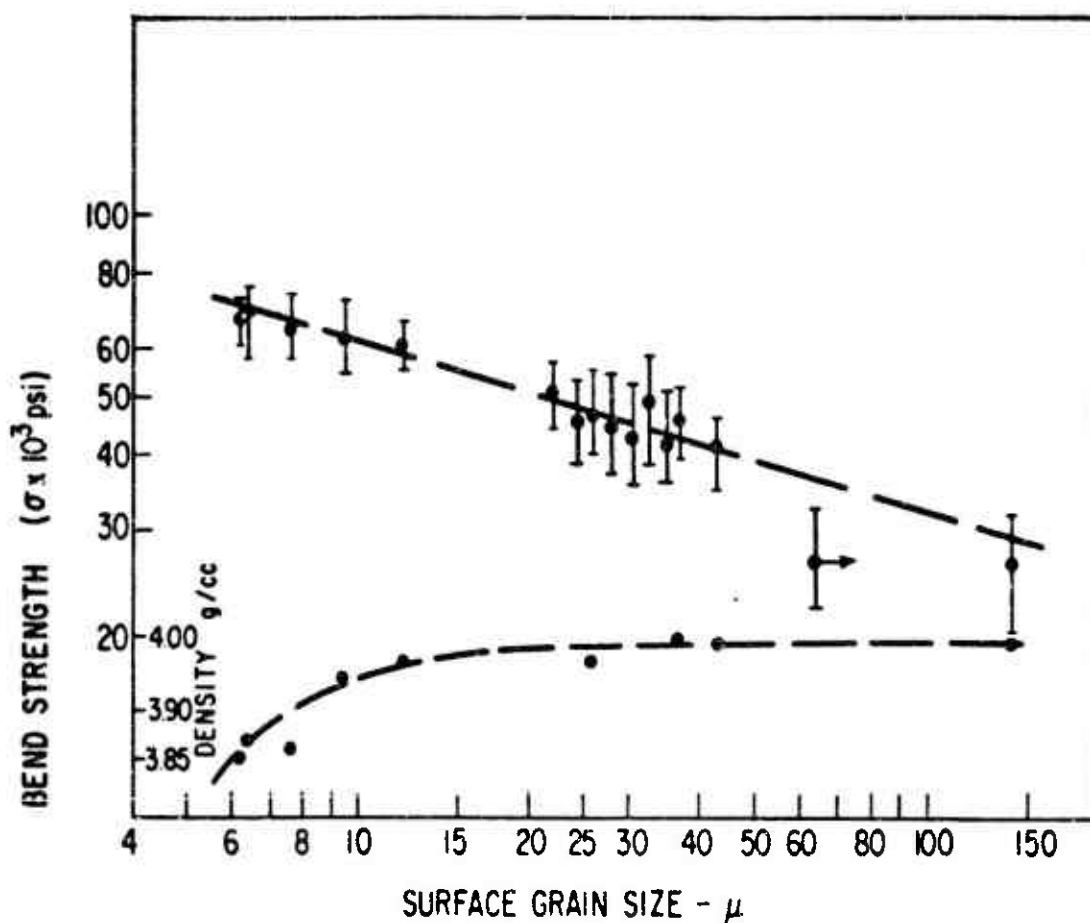
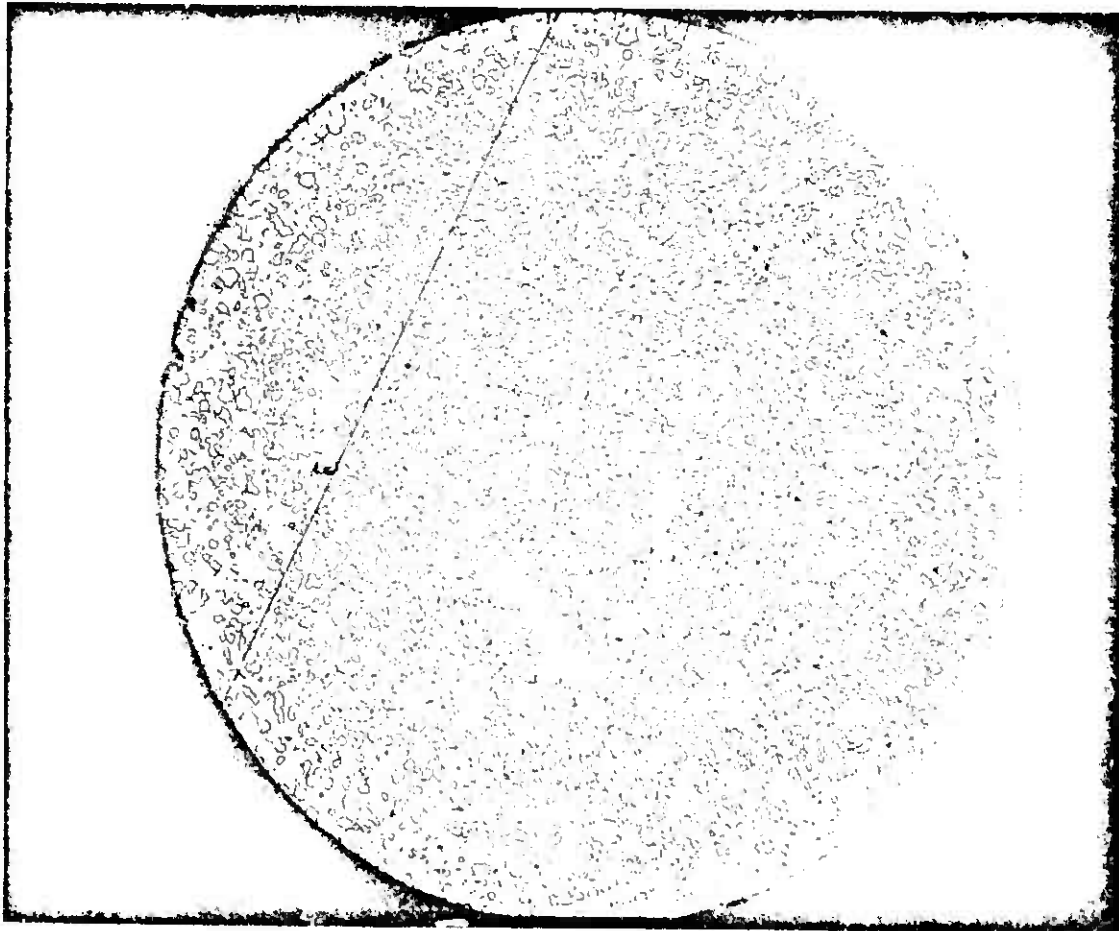


Fig. 12 Bend strength and density of Lucalox alumina extruded rods as a function of surface grain size.

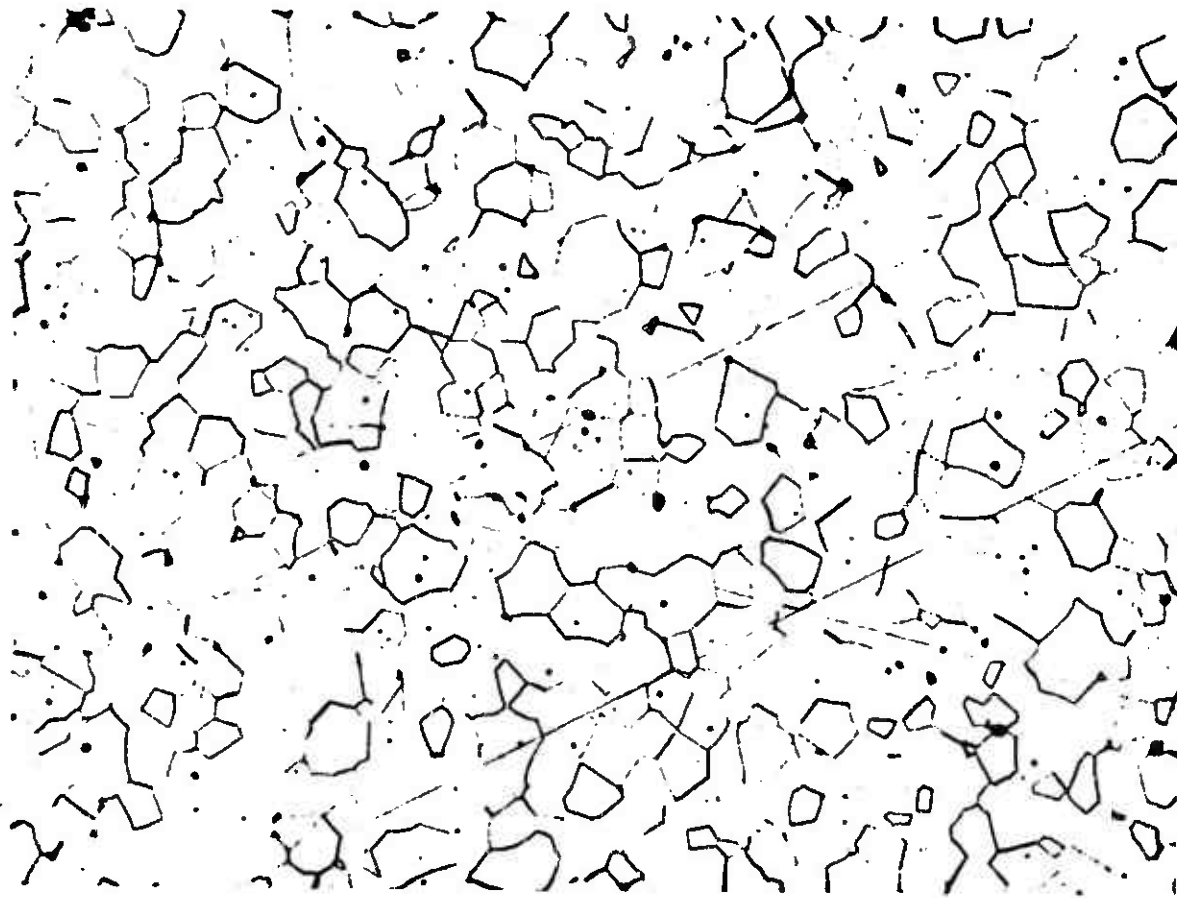
in the handling of data, the nominal grain size of this batch was computed from lineal analysis measurements as before, and was plotted accordingly. The standard material selected for use throughout the major portion of the fatigue work ranged 30 to 40 microns in grain size with a corresponding bend strength of about 45,000 psi under the cited conditions. The microstructure of this standard Lucalox alumina is presented in Fig. 13.

Figure 14 illustrates the effect of grain size and testing rate on the strength of the polycrystalline alumina specimens from which the standard Lucalox alumina for this investigation was selected. This figure also includes the strength-grain size dependence for tests at liquid nitrogen temperature. Even with these results it is clear that a fatiguing effect operates for, in general, the strength of the specimens tested in air at a strain rate of  $2.7 \times 10^{-4}$  is approximately 20 per cent



75X

(a)



(b)

500X

Fig. 13 Microstructure of standard Lucalox alumina test material (average surface grain size of 30 to 40 microns); (etchant- $\text{H}_3\text{PO}_4$ , 10 minutes). [Overetching of grain boundaries has occurred in (b).]

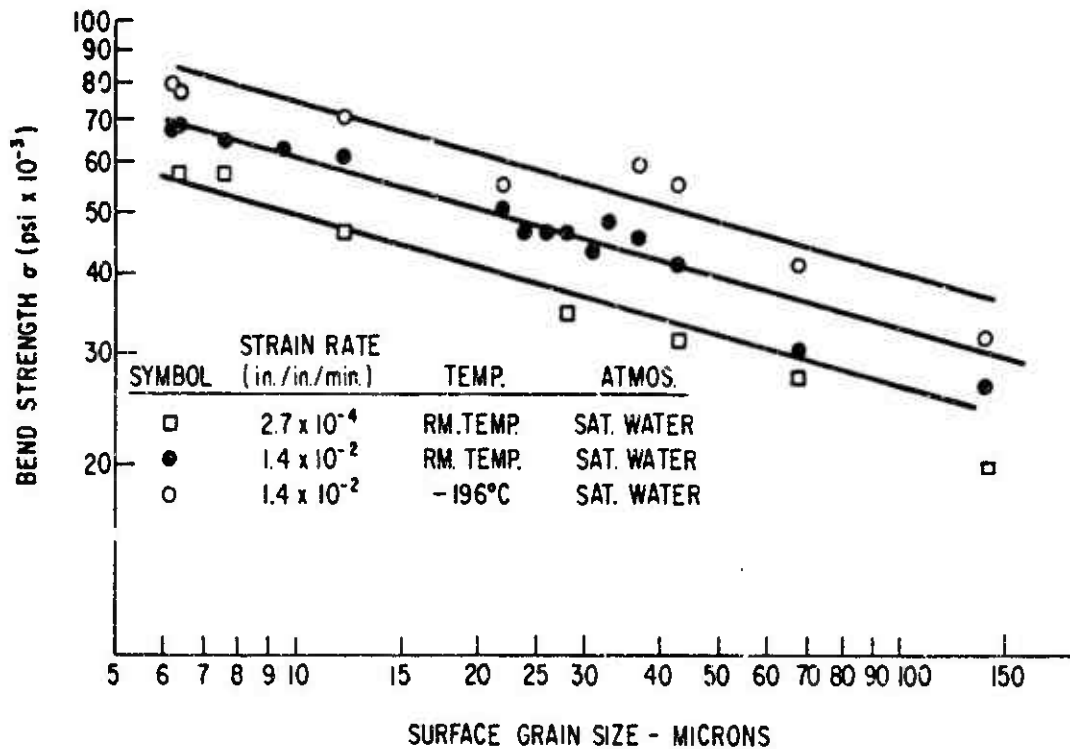


Fig. 14 Effect of surface grain size, loading rate, and temperature on the bend strength of Lucalox alumina.

less than that tested at a strain rate of  $1.4 \times 10^{-2}$  and 30 percent less than the base level strength determined at liquid nitrogen temperature. Within the limits of accuracy of the data it would appear that although grain size affects the base level strength, it does not alter the fatigue effects that are observed.

## 2. Constant Strain-rate Tests on Standard Polycrystalline (Lucalox) Alumina

A calculated strain rate of  $2.7 \times 10^{-4}$  in/in/min on the outer tensile fiber was selected for the bend tests. Figure 15 presents the bend strength behavior of this material in the same temperature-atmosphere conditions as for sapphire.

It can be seen that this behavior is somewhat similar to that of sapphire, in that the bend strength decreases in the order vacuum, dry hydrogen, and wet hydrogen atmospheres. Again, the curves become indistinguishable around 850°C showing that corrosion/fatigue effects have largely disappeared.

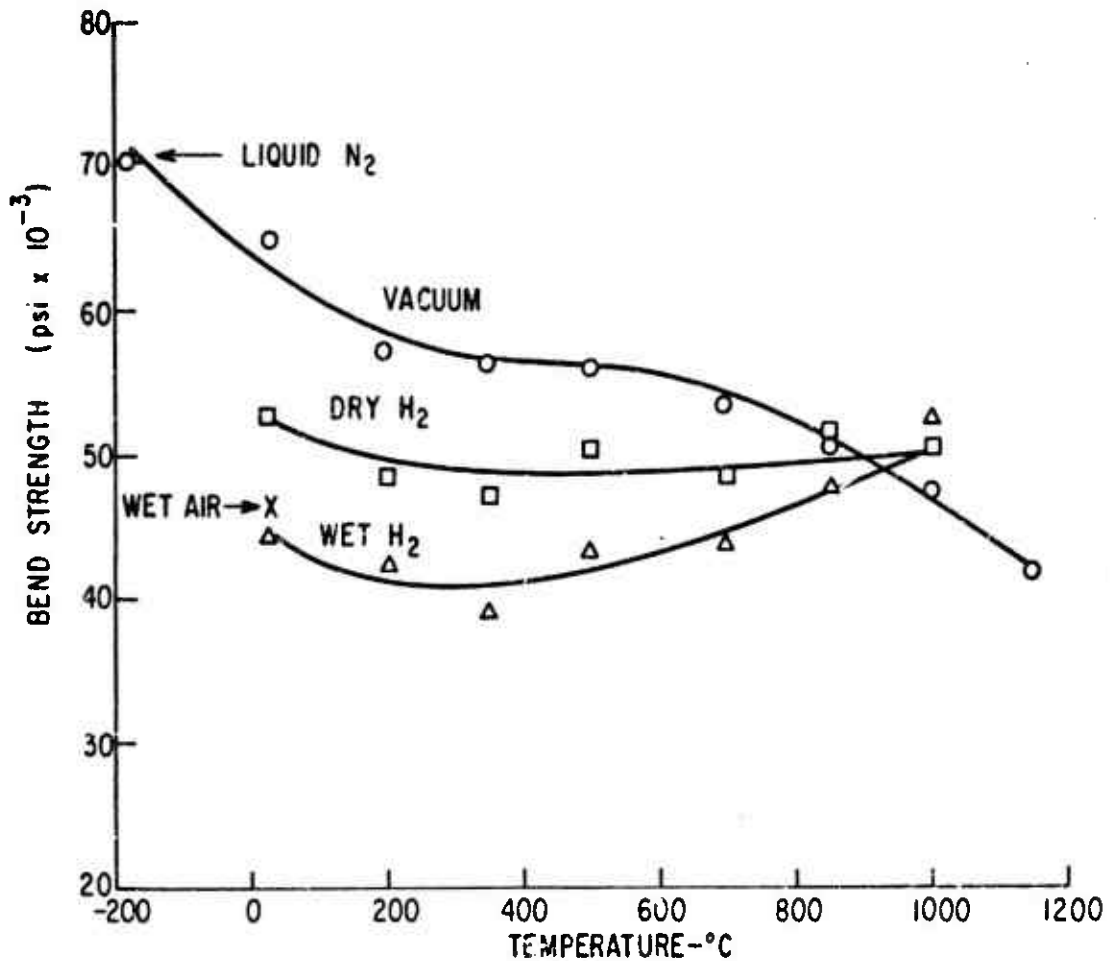


Fig. 15 Temperature-atmosphere effects on the bend strength of standard Lucalox alumina specimens.

Figure 16 illustrates the normalized vacuum strength of Lucalox alumina as a function of temperature, compared with the normalized Young's modulus of polycrystalline alumina over the same temperature range. A similarity of the curves suggests that the falloff of strength of alumina in vacuum with increased temperatures may possibly be attributed to the changes in theoretical strength as reflected by the changes in modulus with increased temperature.

A slight curvature in the load-time plots at the highest temperature used (1150°C) raised the question of whether or not plastic deformation of the polycrystalline samples was occurring. Plastic deformation may take place by grain boundary sliding or by the Nabarro-Herring stress-induced diffusion mechanism; for the latter, Folweiler<sup>(24)</sup>

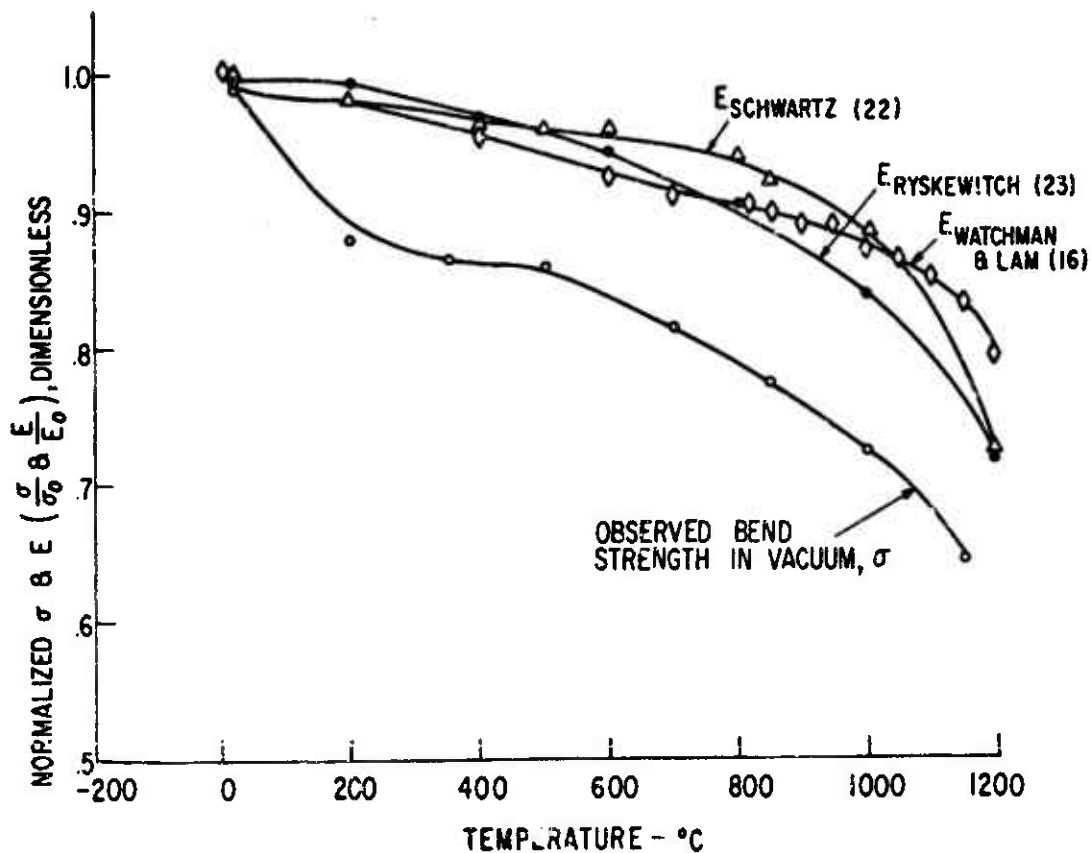


Fig. 16 Lucalox alumina vacuum bend strength and Young's modulus vs temperature.

has calculated the oxygen diffusion coefficient over the temperature range 1400° to 1800°C. Extrapolation of these data yields a diffusion coefficient of about  $10^{-15}$  cm<sup>2</sup>/sec at 1150°C; however, the coefficient as calculated from the experimental data in this report, assuming plastic flow occurs, yields a diffusion coefficient of about  $10^{-11}$ , which is absurdly high. Therefore, the observed curvature is very probably only that associated with the metal parts of the fixture, and no plastic flow of the alumina is occurring. The presence of the curvature, however, means that the strain rate is being changed, and no further tests were done at this temperature.

Both bend strength and Young's modulus are seen to decay quite rapidly in this high-temperature region. This is in marked contrast to the behavior of single-crystal sapphire, whose apparent bend strength increases rather than decreases at these temperatures, and whose modulus remains linear. The strength increase of sapphire

can be explained qualitatively on the basis of local stress relief by basal slip, well known to operate at these temperatures and strain rates. Presumably, polycrystalline material shows increased viscous characteristics with increasing temperature.

### 3. Delayed Failure Tests on Lucalox Alumina

Table V presents time-to-failure data at several temperatures. It is seen that again the data, while not extensive, are analogous to that of sapphire, with times-to-failure being strongly related to stress level and atmosphere at each temperature. It was felt that work on the standard single-crystal specimens would be of more basic concern, so the major emphasis of the delayed-failure investigation was put on these.

TABLE V

Static Fatigue Data on Standard Lucalox Alumina Specimens

Constant Stress (psi)	Conditions	No. Specimens Failing Within Indicated Time Decades (minutes)								Most Prob. Time-to-failure (min)
		10 <sup>1</sup>	10 <sup>2</sup>	10 <sup>3</sup>	10 <sup>4</sup>	10 <sup>5</sup>	10 <sup>6</sup>	10 <sup>7</sup>	<10 <sup>8</sup>	
55, 100 psi	Room Temp. Rough Vacuum (10 mm Hg)	10	6	4	3	3	6	2	3	~ 10 <sup>-1</sup>
48, 000 psi	As above			1			3	2	7	
44, 100 psi	As above							2	2	
48, 50 psi	Room Temp. Air, 20% RH	2		1	2	1	1			
48, 500 psi	198°C. 200 psig steam	10								~ 0
41, 600 psi	As above	3	1	1	3	1				
29, 600 psi	As above								2	6

## DISCUSSION OF EXPERIMENTAL RESULTS

### Fatigue Failure Theory

Charles and Hillig<sup>(25)</sup> have presented a theory for static fatigue of isotropic brittle materials in which the material is considered as an elastic continuum which chemically reacts with its environment. Failure of the material under load is attributed to the alteration, by a corrosion or dissolution reaction, of the geometries of pre-existing flaws or cracks on the surface.

The well-known "Joffe effect" is concerned with the blunting or rounding out of surface flaws by etching or dissolution. By this process the effectiveness of surface flaws as stress concentrators is reduced,

and the solid will withstand a larger than usual load before rupture. It is not generally recognized, however, that if the rate of etching or dissolution is sensitive to the stress state, as well as the chemical conditions existing around a flaw or crack, sharpening of the crack with time is a possible consequence and catastrophic failure will result. The failure time depends on the magnitude of the applied stress, the duration of exposure to a reactive environment, and parameters characteristic of the material.

The model examined by the above authors consisted of an element of material under uniaxial stress and containing a semi-elliptical surface flaw. The material was considered to be immersed in a reactive environment such that, under zero stress, the thermally activated reaction rate of a plane surface would be given by an Arrhenius equation of the following form:

$$v'' = v_0 \exp - A/RT \quad (1)$$

where  $v''$  = rate of penetration of the solid-reaction product plane interface

- $v_0$  = a constant
- $A$  = an activation energy
- $R$  = gas constant
- $T$  = absolute temperature.

The reaction rate of a curved surface differs from that of a plane surface and since the curvatures associated with stress concentrating flaws are very large the effect must be considered. Thus, for a curved surface, Eq. (1) took the following form:

$$v' = v_0 \exp -[A + \Gamma V_M/\rho]/RT \quad (2)$$

where  $v'$  = rate of penetration of the solid-reaction product curved interface

- $\Gamma$  = surface free energy between the solid and the reaction product
- $V_M$  = molar volume of solid material
- $\rho$  = radius of curvature of the interface.

Many kinetic processes in solids (diffusion, ionic conductivity) are affected by hydrostatic pressure in a manner that indicates that the activation energies for the processes are linearly related to the applied pressure. The proportionality constant is termed an activation volume

and has typical values of a few  $\text{cm}^3/\text{mole}$  of reacting species. The assumption is made that such a description of the effect of stress on the reaction rate model under discussion is adequate. Thus the local velocity  $v$  of corrosion or dissolution normal to the solid surface is expressed by:

$$v = v_0 \exp - [A - V^* \sigma + \Gamma V_M / \rho] \quad (3)$$

where  $V^*$  is the activation volume and  $\sigma$  the local stress.

Starting with a flaw of known geometry, one can apply the Inglis<sup>(26)</sup> theory and determine the stress distribution around the contour of a flaw. Equation (3) may then be utilized to set up a differential equation expressing the change of the flaw contour with time. It is evident that a change in flaw contour leads to a change in stress distribution which in turn modifies the rate of change of flaw contour. Thus, depending on the relative values of the parameters involved, a number of possibilities exist for the progress of the flaw with time. Figure 17 illustrates these possibilities. If the applied stress is sufficiently high, the change of stress concentration of the flaw with time ( $\partial u / \partial \tau$ ) may be positive and the flaw will sharpen and lead to specimen failure [Fig. 17(a)]; if the applied stress is low the change of stress concentration with time may be negative and the flaw will round out and the specimen may appear to strengthen [Fig. 17(c)]. At some intermediate applied stress the sharpening of the flaw by stress corrosion may just balance the rounding out effect and the stress concentration of the flaw may remain constant [Fig. 17(b)].

It is evident that a theory, as proposed above, is of little value unless it is applicable to cracks or flaws which differ in initial configuration. In the testing of brittle solids, a measure of the initial severity of a flaw may be obtained by testing under conditions whereby

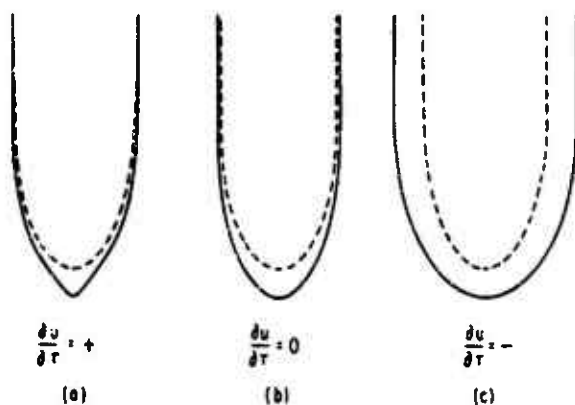


Fig. 17 Hypothetical changes in flaw geometry due to corrosion or dissolution: (a) flaw sharpening as a result of stress corrosion; (b) flaw growth such that the rounding of the tip by stress corrosion balances the lengthening of the flaw; (c) flaw rounding by corrosion or dissolution (Joffe effect). (After Charles and Hillig, Ref. 25.)

no alteration, except elastic deformation, of the flaw occurs until spontaneous propagation takes place. It is felt that, experimentally, testing at liquid nitrogen temperatures satisfies these conditions for most materials. Further, the comparison of the initial configuration of a flaw with its configuration at a later time, just prior to spontaneous propagation, is of little practical interest. What is of practical interest, however, is the failure stress of a material when flaw growth is prevented as compared to the failure stress of the material when flaw growth, by stress corrosion and prior to spontaneous propagation, occurs. Because of the direct relationship between flaw configuration and failure stress, it is probably evident that a comparison of a failure stress,  $S$ , obtained under arbitrary conditions, with a failure stress,  $S_N$ , obtained under liquid nitrogen temperatures is nothing more than a comparison of final and initial configuration of a flaw subject to alteration by corrosion.

It is for this reason that the static fatigue equations for failure time as a function of stress, developed by the previously mentioned authors, do not require any further knowledge of the geometries of flaws than their initial depths.

The basic equations which are a result of the above theory are given as follows:

$$S_L = \left[ \frac{3 \sigma_{th} \Gamma V_M}{8 V^* L} \right]^{1/2} \quad (4)$$

where  $S_L$  is the fatigue limit stress, or the applied stress below which no failure of the specimen can occur [condition (b) in Fig. 17],  $\sigma_{th}$  is the theoretical strength of the material and  $L$  the initial depth of the flaw. The other terms have previously been defined. In Eq. (5):

$$\ln(t/t_{0.5}) \approx - \frac{V^*}{RT} \sigma_{th} \left[ \frac{S}{S_N} - 1/2 \right] - f(S/S_N) \quad (5)$$

$t$  is the time-to-failure,  $t_{0.5}$  is the time-to-failure at one-half the liquid nitrogen applied stress and  $f(S/S_N)$  is a slowly varying function which relates the short time behavior of a fatigue system to the time behavior of the system as it approaches the fatigue limit. Figure 18 illustrates the essential characteristics of Eq. (5).

In order to evaluate the parameters that control fatigue in a given system it is evident, from an examination of Fig. 18, that fatigue measurements be made in the range near the fatigue limit so that the

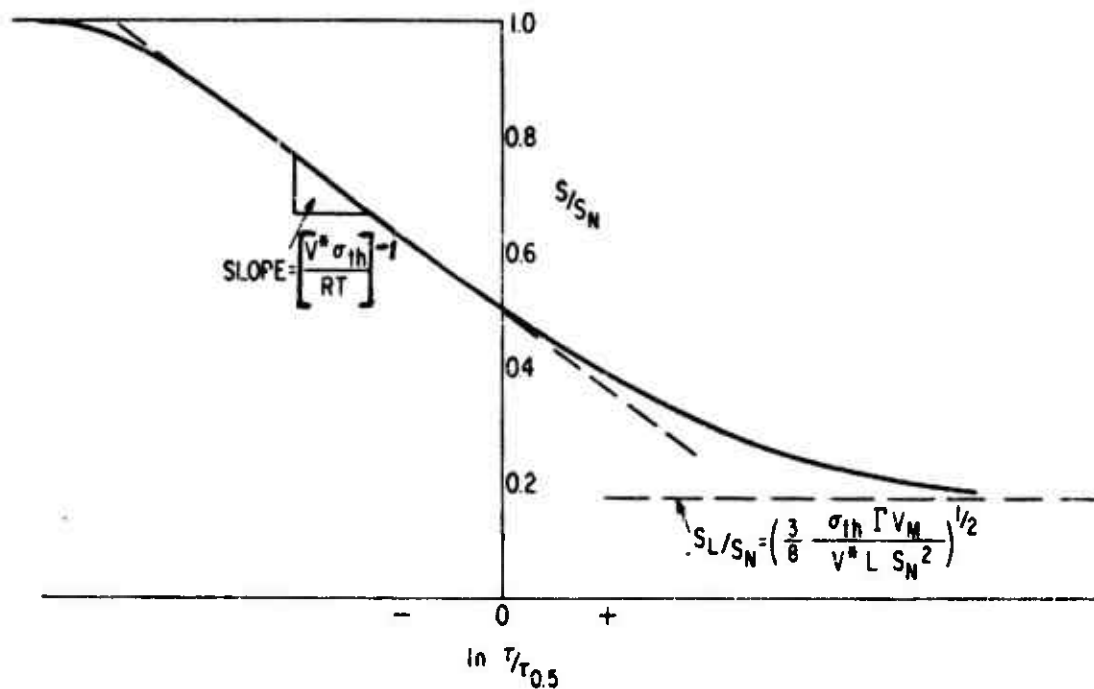


Fig. 18 Schematic fatigue curve (after Charles and Hillig, Ref. 25), where  $\tau$  is time-to-failure and  $\tau_{0.5}$  is the time-to-failure for a stress  $S_n/2$ .

ratio  $S_L/S_N$  may be estimated and further measurements be made in the range  $1 > S/S_N > 0.5$  to determine the slope  $d \ln t / d(S/S_N)$ . Substitution of reasonable values for the theoretical strength of the material, the molar volume, and the initial lengths of cracks then allows calculated estimates of the surface energy,  $\Gamma$ , and the activation volume,  $V^*$ .

As has been previously mentioned, the above theory was developed for an isotropic solid. Even though single-crystal alumina is anisotropic, it was felt that the application of the above theory to the material at hand might prove worthwhile if reasonable  $\Gamma$  and  $V^*$  values were obtained from experimental results.

#### Application of the Fatigue Theory to Low Temperature Tests on Alumina

##### 1. Single-Crystal Alumina

The data for low-temperature fatigue of sapphire in saturated water atmosphere were plotted in Fig. 11, in accordance with the plotting procedure illustrated in Fig. 18.

It is noted that the fatiguing characteristics of sapphire in a water-containing atmosphere are sufficiently extensive that a test temperature as low as  $-35^{\circ}\text{C}$  was required in order that the material withstand stresses of the order of 0.5 to 0.7 the liquid nitrogen failure stresses for measurable lengths of time (0.01 to 10 minutes). The slope of the line passing through the  $-35^{\circ}\text{C}$  data in Fig. 11 is approximately -0.1. Thus,  $d \ln t / d(S/S_N) \approx - \frac{V^* \sigma_{th}}{RT} \approx -10(2.3)$ . The modulus of elasticity,  $E$ , of sapphire at this temperature is approximately  $3.6 \times 10^5 \text{ kg/cm}^2$  and thus one would estimate the theoretical strength,  $\sigma_{th}$ , of sapphire as about  $E/5$  or  $7 \times 10^5 \text{ kg/cm}^2$ . Using this value the activation volume for the corrosion reaction resulting in fatigue of sapphire is about 0.66 cc/mole (referred to a uniaxial stress). This result compares with such typical values as the activation volume for carbon in iron (referred to a hydrostatic stress) which is about 0.5 cc/mole, and the activation volume for alkali metal ion diffusion in silicate glasses (referred to a hydrostatic stress) which is about 4.0 cc/mole.

Referring once more to Fig. 11 it is noted that the fatigue data, at a test temperature of  $200^{\circ}\text{C}$ , appears to approach a fatigue limit of about  $S_L/S_N \approx 0.2$ . This value is only slightly higher than that for typical glasses, i. e., about 0.15. (25) Using Eq. (4), a value of the molar volume of sapphire of about 25 cc and the previously estimated values of  $\sigma_{th}$  and  $V^*$  the ratio  $\Gamma/L$  calculates to be approximately  $10^5$ . Thus, for a 2-micron-long crack  $\Gamma$  is about  $20 \text{ ergs/cm}^2$ . Since  $\Gamma$  is the surface energy between alumina and its hydrated corrosion product, it would certainly be much lower than the surface energy between alumina and vacuum, which is variously estimated to be between 1000 and 2000  $\text{ergs/cm}^2$ . The above value for  $\Gamma$  may be low but is perhaps correct to within an order of magnitude.

In Eqs. (1) to (3) the factor,  $A$ , is defined as the activation energy for the chemical reaction which results in the static fatigue of alumina. In Table IV it will be noted that sapphire rods underwent static fatigue tests in saturated water vapor at two different temperatures ( $-35^{\circ}$  to  $25^{\circ}\text{C}$ ) at equal applied bending stresses of 34,400 psi. This applied bending stress corresponded to an  $S/S_N$  value of 0.48. The estimated failure time for the specimens at room temperature was one second whereas the failure time, under the same load, at  $-35^{\circ}\text{C}$  was estimated at 7 minutes. By utilizing these data an estimate of the quantity  $A$  may be made, i. e.:

$$\log \frac{7(30)}{1} = \frac{A}{2.3R} \left( \frac{1}{238} - \frac{1}{298} \right)$$

From the above  $A$  calculates to be about 14 kcal/mole. This value is reasonable for the activation energy for a low-temperature hydration reaction of an oxide like alumina.

## 2. Polycrystalline Alumina

Insufficient experimental results on the low-temperature static fatigue of Lucalox alumina were obtained to draw definitive comparisons between its fatigue behavior and that of sapphire. It is noted, however, by reference to Table V, that most of the failure times for applied stresses of 29,600 psi under saturated water vapor at 200°C were in excess of  $10^4$  minutes. The fatigue limit stress for Lucalox alumina must therefore be approximately this value. Since the liquid nitrogen bend strength of these particular samples was about 90,000 psi the fatigue limit ratio,  $S/S_N$ , would be about 0.33. It is of interest that this value is considerably higher than that obtained for single crystal alumina under similar conditions, i.e., 0.2. From these data it is concluded that the low-temperature fatiguing behavior of polycrystalline alumina is not as severe as that for sapphire. The presence of grain boundaries and the small MgO addition in Lucalox alumina would, in all probability, lead to a difference in the corrosion behavior between Lucalox alumina and sapphire. From this it would follow that the fatigue behaviors would also differ. Whether, under the above fatigue theory, one would attribute this difference to a change in the activation volume for the corrosion reaction or to a difference in the interfacial surface energy values, cannot be resolved at this time. In all probability both factors are sensitive to the compositional and structural characteristics of the two materials.

That fatigue of Lucalox alumina occurs under constant strain rate conditions is shown by the data in Fig. 14. Under constant environmental conditions a lowering of the strain rate results in a lowering of the rupture stress, and this effect is independent of grain size. Further, at liquid nitrogen temperatures where corrosion cannot be a weakening factor, the highest rupture strengths are obtained.

With reference to Fig. 14 one concludes that the fatigue mechanism in Lucalox alumina is not affected by constitutional variables such as the grain size of the material. This conclusion follows from the fact that the relative reduction in strength from the base level value of the Lucalox alumina to the level obtained at room temperature under a small strain rate is independent of the grain size. It is well to elaborate somewhat on this point, for within the initial planning of that phase of the over-all program assigned to Task 9 consideration was given to the manner in which the data obtained on the special samples required by Task 9 could be correlated with data on different samples used by other investigators in the program. The necessary correlation proves to be relatively simple and results from the following argument. The intrinsic strength of an actual brittle ceramic body is controlled by those factors that determine the theoretical strength of the material from which the body is composed

and the geometry of that particular surface flaw which is subjected to the most severe stress conditions. Failure occurs when the stress at the tip of this flaw reaches the theoretical strength of the material. Thus the intrinsic strength of the body is subject to constitutional variables such as grain size and distribution, surface treatment, and the area of sample under stress as well as the variables introduced by test arrangements. As has been shown in the previous data, the intrinsic strength of an alumina specimen, of arbitrary preparation and shape, may be reduced if the environment permits a fatigue reaction. Prevention of this fatigue reaction by testing at reduced temperature, however, allows a measurement of the intrinsic or base-level strength of this specimen. Since the data already obtained (Fig. 11) indicate that the maximum reduction of the intrinsic strength of alumina by corrosion fatigue is approximately 80 per cent one can, in principle, obtain the approximate fatigue level stress of any specimen of alumina, tested in a water-containing atmosphere, by first determining the intrinsic or base-level strength at low temperature.

### The High-Temperature Fatiguing Characteristics of Alumina

#### 1. Single-Crystal Alumina

Figure 9, which is a summary of all the constant strain rate bend tests performed on sapphire rods, indicates that the sapphire specimens were markedly strengthened by a prior anneal at high temperature, but irrespective of the initial states of the specimens, testing in various atmospheres showed a fatiguing effect which, to a limit, became more severe with increasing temperature. As has been mentioned previously other investigators have shown the trend to decreasing strengths as temperature is increased. In the present tests, however, it is seen that a wet atmosphere has the most pronounced fatiguing effect and vacuum ( $10^{-5}$  mm Hg) has the least. The dry hydrogen tests are somewhat inconclusive for it was found after the experiments that the quoted dewpoint of the hydrogen was not as low as initially expected ( $-30^{\circ}\text{C}$ ). In any event for both the annealed and as-received specimens the difference in failure behavior in different atmospheres must be interpreted as an atmosphere effect. This difference diminishes with increasing temperature, until, at a temperature of about  $850^{\circ}\text{C}$ , no atmosphere effect on the failure strengths can be observed. As has been mentioned previously, the upturn of the failure strength curves at temperatures in excess of  $850^{\circ}\text{C}$  is probably due to a plastic flow process.

The question remains as to whether or not the initial drop off in strength of the vacuum tested specimens up to the  $600^{\circ}$  to  $800^{\circ}\text{C}$  range

should be attributed to a residual atmosphere and therefore a corrosion effect. Such an explanation may be entirely reasonable for a vacuum of  $10^{-5}$  mm Hg must be considered as still relatively reactive. Because of this ambiguity, five annealed sapphire specimens were tested at the end of the program at a temperature of  $500^{\circ}\text{C}$  in a positive pressure atmosphere of nitrogen gas derived solely from gas evaporated from liquid nitrogen. As far as water vapor was concerned this atmosphere would be considered dry, yet the failure stresses were no different than those previously obtained under a vacuum of  $10^{-5}$  mm Hg. This last experiment indicates that a water reaction cannot be responsible for the strength dropoff with temperature of the vacuum tested specimens. This experiment also suggests that sapphire decreases in strength as temperature is raised to about  $850^{\circ}\text{C}$  and that this strength decrease is a consequence of temperature alone.

## 2. Polycrystalline Alumina

Figure 15 shows the effect of atmosphere on the bend strength of Lucalox alumina. Once again the vacuum tested specimens are stronger than the wet hydrogen tested specimens until a temperature of about  $900^{\circ}\text{C}$  is reached where no atmosphere effect remains. Thus it must be concluded that evidences of corrosion fatigue resulting from water vapor may be obtained in the testing of Lucalox alumina to a relatively high temperature. As might reasonably be expected, Lucalox alumina shows no evidence of strengthening by plastic flow at as low a temperature as observed for sapphire.

## CONCLUSIONS

The results reported in previous sections confirm and extend previous investigator's findings that alumina, both in single and polycrystalline form, is subject to static fatigue. From these results a number of general conclusions may be made:

1. The reaction responsible for fatigue near room temperature is probably one in which water vapor from the atmosphere combines with the alumina to form one or more of the many possible hydrated states of alumina. The reduction in strength of sapphire and polycrystalline alumina specimens due to corrosion fatigue can be as high as 70 to 80 per cent of their intrinsic strengths.

2. In mechanical tests, the fatigue process in alumina manifests itself in the same fashion as is observed for other materials (e.g., glass). First, one observes delayed failure of alumina specimens at constant load in which the most probable failure time is a very strong function of

the applied stress, atmosphere, and temperature. Second, the failure stress at a constant loading rate increases with the absolute value of the loading rate (Fig. 14). Third, the coefficient of variation of failure stresses of samples subjected to similar mechanical testing procedures is considerably less when the fatigue process is permitted than when it is prevented. This situation is illustrated by the data in Table VI in which the coefficient of variation for mechanical tests at liquid nitrogen temperature or in vacuum (fatigue process prevented) is considerably higher than that obtained in mechanical tests in wet hydrogen or air at moderate temperatures (fatigue process permitted). Fourth, the fracture behavior of single crystals at a given temperature depends on the atmosphere present during the test. Mirror fracture surfaces, characteristic of delayed failure fractures, appear only when humid conditions obtain. Under other conditions, interrupted cleavage or parting on definite crystallographic planes is the rule.

TABLE VI

Low-Temperature Bend Strengths and Coefficients of Variations of Standard Lucalox Alumina Specimens

$$\dot{\epsilon} = 3 \times 10^{-4} \text{ in/in/min}$$

N = number of tests

$\sigma$  = average failure stress  $\times 10^3$  psi

v = coefficient of variation

Temp (°C)		Sat. Air	Dry H <sub>2</sub>	Wet H <sub>2</sub>	Vacuum	Liq. N <sub>2</sub>
-196	N					20
	$\sigma$					66.5
	v					13.2%
RT	N	11	11	10	11	
	$\sigma$	46.5	52.3	44.9	65	
	v	5%	5.9%	6.8%	9%	
200	N		11	9	34	
	$\sigma$		48.4	42	57.2	
	v		7.8%	7.4%	12.8%	

3. The application of a fatigue theory to the low temperature fatigue data for sapphire and polycrystalline alumina resulted in values for the activation volume (0.66 cc/mole), the surface energy between alumina and its hydration product (less than one-hundred ergs/cm<sup>2</sup>) and the activation energy for the hydration reaction (14 kcal/mole) which are reasonable for a stress corrosion reaction.

4. The observed bend strength of sapphire single crystal is quite sensitive to its prior thermal history. In this investigation, heat-treating as-received ground rods improved their low-temperature strength in all atmospheres by about 50 per cent, up to about 500°C. The atmosphere present during heat-treatment at 1125°C has no noticeable effect on the low-temperature bend strength.

The mechanism by which this strengthening occurs is unknown, but the fact that annealing has less of an effect on samples in which the base planes are at 0° to the longitudinal axis of the rod specimens, than on samples whose base planes are at 60° to the rod axis, suggests that surface preparation (grinding) may introduce more surface flaws on the latter specimens and that these flaws heal under the annealing treatment.

5. With an essentially inert gas (H<sub>2</sub>) saturated with water vapor at room temperature, the fatigue reaction in both Lucalox alumina and sapphire is sufficiently strong to give evidence of fatigue up to temperatures approaching 850°C.

6. Superimposed on the atmosphere fatiguing process of sapphire, which operates up to about 850°C, appears to be a further weakening process of equal severity which may depend only on temperature and not on atmosphere. Whether or not such an effect truly exists can only be determined by very exacting experiments.

7. Strengthening of sapphire by plastic deformation is observable at temperatures as low as 900°C. Evidences for plastic deformation in Lucalox alumina at temperatures below 1100°C were not obtained.

#### ACKNOWLEDGMENTS

The authors wish to acknowledge assistance in the program from a number of sources. A. G. Pincus, J. W. Szymazek, A. Garufy, and H. Lockwood of the GE Research Lab. Process Laboratories Unit produced the polycrystalline Lucalox alumina samples. M. C. Houle prepared the photomicrographs used in the grain-size determinations. D. C. Lord and W. E. Rollins, of the Mechanical Testing Laboratory, obtained much of the bend strength data. L. M. Osika of the X-ray Diffraction Laboratory performed the x-ray work during the program. Discussions with J. E. Burke, W. B. Hillig, M. L. Kronberg, L. Navias, R. C. DeVries, and C. A. Bruch were most helpful and stimulating.

## REFERENCES

1. J.P. Roberts and W. Watt., "Mechanical Properties of Sintered Alumina," Ceram. Glass, 10, 53 (1952).
2. J.B. Wachtman, Jr. and L.H. Maxwell, "Plastic Deformation of Ceramic-Oxide Single Crystals," J. Am. Ceram. Soc., 37 (7), 291-99 (1954).
3. L.S. Williams, "Stress-Endurance of Sintered Alumina," Trans. Brit. Ceram. Soc., 35, 287-312 (1956).
4. S. Pearson, "Delayed Fracture of Sintered Alumina," Proc. Phys. Soc. (London), 69(B), 1293-96 (1956).
5. S.S. Brenner, "Mechanical Behavior of Sapphire Whiskers," J. Appl. Phys., 33 (1), 33-39 (1962).
6. R.J. Charles, "The Strength of Silicate Glasses and Some Crystalline Oxides," p. 225-249 in Fracture, John Wiley and Sons, Inc., New York (1959).
7. F.P. Clarke, private communication.
8. M.V. Klassen-Nekhlyudova, as reported in Oxide Ceramics, E. Ryshkewitch, Academic Press, New York, (1960), p. 155; see also "Dependence of the Strength of Corundum Crystals on Crystallographic Orientation During Testing in Bend and Tension," Physical Properties of Synthetic Corundum, A Symposium, Trudy Inst. Krist. Akad. Nauk USSR, No. 8, p. 215-224 (1953).
9. A.K. Seemann, "Gems, Synthetic," Encyclopedia of Chemical Tech. 7, (1951), p. 162; "Alumina Properties," Technical Paper No. 10, Alcoa Research Labs, (1960).
10. J.B. Wachtman, Jr. and L.H. Maxwell, "Plastic Deformation of Ceramic Oxide Single Crystals III," J. Am. Ceram. Soc., 40 (11), 377-85 (1957).
11. R.P. Steijn, "On the Wear of Sapphire," J. Appl. Phys., 32 (10) 1951-58 (1961).
12. E.A. Jackman and J.P. Roberts, "On the Strength of Polycrystalline and Single Crystal Corundum," Trans. Brit. Ceram. Soc., 54, 389-98 (1955).

13. J.B. Wachtman, Jr. and L.H. Maxwell, TR-WADC 53-265 and supplements, Nat. Bur. Stand.(1956), as presented by R.D. Olt, Linde Bulletin F-917-A (1958).
14. G.E. Tomilovski, "Effects of Heat Treating Synthetic Corundum Crystals at 1300°C on Mechanical Properties," Phys. Prop. of Synth. Corun., A Symposium, Trudy Inst. Krist. Akad. Nauk USSR, No. 8, p. 341-54 (1953).
15. M.L. Kronberg, "Dynamical Flow Properties of Single Crystals of Sapphire, Part I," GE Research Lab. Rept. No. 61-GC-197 (December 1961).
16. J.B. Wachtman and D.G. Lam, Jr., "Young's Modulus of Various Refractory Materials as a Function of Temperature," J. Am. Ceram. Soc., 42 (5), 254-60 (1959).
17. J.B. Wachtman, Jr., W.E. Tefft, and D.G. Lam, Jr., "Young's Modulus of Single Crystal Corundum from 77 to 850° K", Chap. 15 in Mechanical Properties of Engineering Ceramics, Kriegel and Palmour, eds., Interscience, New York, N.Y. (1961), p. 221-223.
18. E.M. Pigolina and V.V. Svyatuklin, "An Investigation of the Parting Planes of Synthetic Corundum by Optical and X-ray Methods," Phys. Prop. Syn. Corun., A Symposium, Trudy Inst. Krist. Akad. Nauk USSR, No. 8, p. 299-308 (1953).
19. H. Winchell, "Orientation of Synthetic Corundum for Jewel Bearings," Am. Mineralogist, 29, 399-414 (1944).
20. N.J. Petch, "Effect of Surface Energy on Brittle Behavior," p. 279, Final Report, "Studies of the Brittle Behavior of Ceramic Materials," N.A. Weil, ed., ARF 8203-16 (1961).
21. R.L. Fullman, "Measurement of Particle Sizes in Opaque Bodies," J. Met., 5, 447 (1953).
22. B. Schwartz, "Thermal Stress Failure of Pure Refractory Oxides," J. Am. Ceram. Soc., 35 (12), 325-333 (1952).
23. E. Ryshkewitch, Oxide Ceramics, Academic Press, New York, N.Y. (1960), p. 148.
24. R.C. Folweiler, "Creep Behavior of Pore-Free Polycrystalline Aluminum Oxide," J. Appl. Phys., 32 (5), 773-78 (1961).

25. R. J. Charles and W. B. Hillig, "The Kinetics of Glass Failure by Stress Corrosion," Symposium sur la Resistance Mechanique du Verre et les Moyens de l'Ameliorer, Florence, Italy (September 1961).
26. C. E. Inglis, "Stresses in a Plate Due to the Presence of Cracks and Sharp Corners," Proc. Inst. Naval Arc., 55, 219 (1913).

# GENERAL ELECTRIC

## *Research Laboratory*

SCHENECTADY, NEW YORK

### TECHNICAL INFORMATION SERIES

Title Page

<b>AUTHOR</b> Charles, R. J. Shaw, R. R.	<b>SUBJECT CLASSIFICATION</b> strength of materials	<b>NO.</b> 62-RL-3081M <hr/> <b>DATE</b> July 1962
<b>TITLE</b> Delayed Failure of Polycrystalline and Single-Crystal Alumina		
<b>ABSTRACT</b> This work was undertaken to confirm and extend prior work on the static fatigue or delayed failure of alumina ceramics. The investigations were particularly concerned with the effects of water vapor and temperature on the long-term mechanical strengths of these materials. Mechanical tests were therefore made over a large temperature range (-196° to 1100°C) in dry, humid, and		
<b>G.E. CLASS</b> 1	<b>REPRODUCIBLE COPY FILED AT</b> Research Information Section  The Knolls Schenectady, New York	<b>NO. PAGES</b> 39
<b>GOV. CLASS</b>		
saturated atmospheres.  Both single-crystal sapphire and polycrystalline alumina exhibited strong delayed failure characteristics which depended on atmosphere, temperature, and strain rate. Delayed failure was absent at liquid nitrogen temperatures, most readily observable around room temperature and decreased with further increases of temperature until at 900°C it was no longer observable. A very rapid decrease of observed strength of the ceramics with increasing temperature (to 900°C) was observed. This reduction in strength, however, cannot presently be attributed to a corrosion fatigue effect.  A fatigue theory involving stress corrosion of an elastic continuum has been applied to the low-temperature  (continued on back)		

By cutting out this rectangle and folding on the center line, the above information can be fitted into a standard card file.

INFORMATION PREPARED FOR:

SECTION: Ceramic Studies

DEPARTMENT: Metallurgy and Ceramics Research

Abstract (continued)

experimental data on sapphire. Reasonable values for the parameters involved in the theory were obtained.